Journal of Applied Polymer Science

Cellulose nanofibers produced from various agricultural residues and their reinforcement effects in polymer nanocomposites

Alexander Sinclair [1], Long Jiang,[1,2] Dilpreet Bajwa,[1] Sreekala Bajwa,[3] Siwakorn Tangpong,[1] Xinnan Wang[1]

[1]Department of Mechanical Engineering, North Dakota State University, Fargo, North Dakota 58102
[2]Program of Materials and Nanotechnology, North Dakota State University, Fargo, North Dakota 58102
[3]Department of Agriculture and Biosystems Engineering, North Dakota State University, Fargo, North Dakota 58102
Correspondence to: L. Jiang (E-mail: long.jiang@ndsu.edu) and D. Bajwa (E-mail: dilpreet.bajwa@ndsu.edu)

ABSTRACT: Cellulose nanofibers (CNFs) have gained widespread attention due to their extraordinary potential as superior reinforcement to improve physical and mechanical properties of polymer matrix nanocomposites. Biomass residues from local North Dakota represent a potential source for these high value structural constituents. Two types of soybean hull, wheat straw, and softwood flour were subjected to chemical pretreatments followed by mechanical fibrillation to produce CNFs. Atomic force microscopy and scanning electron microscopy results show that nanofibers with uniform diameters in the nanometer range can be easily synthesized. The nanofibers reinforcement potential was then explored via integration of the fibers into a poly(ethylene oxide) polymer matrix. Significant reinforcement effect of the nanofibers was observed from the nanocomposites: tensile modulus and yield strength of the nanocomposites were increased up to 154% and 103%, respectively. The CNFs extracted from the two types of soybean hull and wood flour showed stronger reinforcement (in terms of both modulus and yield strength) than that of the traditional wood pulp based CNFs. The nanofibers extracted from wheat straw showed higher strength but lower modulus compared with those of the traditional CNFs. More work is however needed to improve production reliability/repeatability of the agricultural residue based nanofibers. © 2018 Wiley Periodicals, Inc. J. Appl. Polym. Sci. **2018**, *135*, 46304.

KEYWORDS: biomass; cellulose nanofibers; nanocomposites; TEMPO Treatment

Received 8 August 2017; accepted 27 January 2018
DOI: 10.1002/app.46304

INTRODUCTION

In recent years it has become more of a priority to produce and implement sustainable and environmentally friendly materials.[1] This priority stems from the targeted reductions in petroleum based products and materials. The utilization of renewable or bio-based resources represents a potential solution to many international issues such as petroleum dependence, deteriorating air and water quality, and climate change.[2] Cellulose, as the most abundant natural polymer on the planet, is one of the most studied renewable materials in recent years.[1] Cellulose is mainly found in nature as the primary structural constituent in the primary and secondary walls within plant cells.[3] Cellulose along with hemicellulose, lignin, and pectin, form a naturally occuring biocomposite with its composition varying depending on the source of biomass.[4]

Cellulose is by definition, a complex carbohydrate polymer and can be described as a linear homopolysaccharide consisting of β-1.4-linked anhydro-D-glucose units.[2,5] Cellulose owes its superior mechanical properties to its linearly ordered microstructure. Individual cellulose chains are connected via both intra-molecular and inter-molecular hydrogen bonds resulting from the three hydroxyl groups on each cellulose monomer. This 3D hydrogen bonding network is responsible for the naturally formed linear microfibrils present in the cell walls of lignocellulosic biomass. At their most elementary unit, a microfibril contains 30–40 cellulose chains and have a diameter ranging from 8–50 nm with lengths up to several microns.[6,7]

These elementary fibers have many names and will be referred to as cellulose nanofibers (CNFs) in this study. CNFs have gained widespread research attention due to their many advantageous properties. They are light-weight, strong, biodegradable, sustainable, and relatively inexpensive to produce.[1,2,8] CNFs can be valuable in many applications including high performance composite materials, packaging, electronics, and biomedical applications. CNFs have been shown to provide significant reinforcement potential in many polymer matrix nanocomposites and are summarized in various review articles and books.[4,6,7,9–11]

Worldwide production of lignocellulosic biomass is estimated to be between 10^{10} and 10^{11} metric tons per annum.[2] Approximately 6% is processed by the paper, textile, materials, and chemical industries and is primarily sourced from hard and

softwoods. The remainder of this biomass is produced in the form of agriculture residues and largly goes to waste or low value applications.[2,12] Therefore, deriving CNFs from the agricultral residues of fast growing crops (instead of from trees) is enviromentally and economically advantageous. CNFs from wide variety of non-wood cellulosic biomass have been reported and are summarized in many review articles.[6,7,9,11,13] Non-wood lignocellulosic biomass can be purified and pulped in one third of the time of hard/soft woods and requires less power consumption due to lower lignin contents in the biomass.[13]

Biomass residues readily available in the midwest include corn stalk, wheat straw, soybean hull, flax, as well as many others. CNFs have previously been reported to have been extracted and produced from soybean hull and wheat straw biomasses using novel chemical purification techniques in several previous studies.[8,12,14] The authors of these studies utilized novel purification techniques followed by mechanical fibrillation to produce high quality CNFs. Specifically, the work done by Alemdar *et al.* utilized a patented three step chemical purification approach with alternating alkali and hydrochloric acid soaking.[3,8,12] The first alkaline soak increases the surface area of the ligncellulosic biomass, thus making it more susceptible to acid hydrolysis. Acid hydrolysis was then used to dissolve hemicelluloses present in the biomass. The final alkali soak then broke down the remaining lignin. This technique was reported to have purified the cellulose content of soybean hulls and wheat straw fibers from 43.2% and 56.4% to 84.6% and 94%, respectively.[8]

This work's primary focus is to devise a sustainable pathway for the production of nanocellulose from agricultural residues available in the upper Midwest region of the United States and to evaluate their potential for use in novel nanocomposites. Soybean hull and wheat straw residues will be specifically discussed and compared with more traditionally used softwoods. Modifications made to the documented alkali/hydrolysis used to purify soybean and wheat straw procedure will be discussed. Commercially obtained and purified cellulose from soybean hull biomass will also be utilized and compared to the purified cellulose produced in this study. Additionally, CNFs commercially prepared from bleached Kraft pulp are also used for comparison. To evaluate the reinforcement potential of the produced CNFs, they will be compounded into poly(ethylene oxide) using a solvent casting technique. Solvent casting is a widely reported lab scale process for producing thermoplastic matrix nanocomposites reinforced with CNFs.[15,16] The procedure discussed herein utilizes documented production techniques experimentally modified to produce as good or better results while using locally obtained biomass and modern laboratory equipment.[8,17] The results from this systematic study provide a valuable reference for preparing nanocomposites using CNFs from different biomass resources.

EXPERIMENTAL

Materials

Soybean hull and wheat straw were acquired from local Midwest sources. Pine wood flour was supplied by American Wood Fibers (Schofield, Wisconsin). Fl-1 Soy Fibre, a commercial cellulosic dietary fiber product derived from soybean hulls was supplied from Fibred-Maryland Inc. (Cumberland, MD). Commercial CNFs, produced from wood pulp through a multi-pass high-pressure mechanical grinding process, were acquired from the USDA Forest Products Laboratory (FPL, Madison, WI). 2,2,6,6-tetramethylpiperidine-1-oxy radical (TEMPO), sodium bromide (NaBr), sodium hydroxide (NaOH), sodium chlorite ($NaClO_2$), sodium hypochlorite (NaOCl) solution, and poly(ethylene oxide) (PEO), $M_w = 1{,}000{,}000$ were obtained from Sigma Aldrich (St. Louis, MO) and used without further purification.

Preparation of CNFs

Soybean hull, wheat straw, and pine flour biomass were ground in a laboratory high-speed rotor mill/grinder (Columbia International Tech, Irmo, SC) at a speed of 25,000 RPM followed by screening through U.S. 100 sieve (Pore size 149 μ). The filtrate (fines) were then collected for further cellulose purification.

Isolation of cellulose from soybean hull and wheat straw was performed based on modified method developed in an earlier reported study.[8] Wheat straw and soybean hull fines were first soaked in 2% w/w NaOH solution at 80 °C for 2 h, followed by extensive washing with distilled water (DI). The resulting pulped biomass was then hydrolized by 1 *M* of HCL at 80 °C for 2 h, followed again by washing with DI. The biomass was then soaked in NaOH solution of 2% w/w at 80 °C for 2 h, followed by extensive washing. Washing with DI was carried out via repeated dilution with DI water followed by filtration (Whatman Qualitative 413). The biomass to soluton ratio was 1:10 in each step of the treatment.

Wood flour fines were chemically purified utilizing a bleaching technique.[17] Wood flour fines were bleached successively (5 times) with $NaClO_2$ (0.3 g/g sample) at pH 4–5 and 70 °C for 2 h. Between each succesive treatment, the biomass was washed with DI water to remove residual chemcials and impurities. Washing was again carried out via repeated dilution with DI water followed by filtration (Whatman Qualitative 413). The resulting purified biomass was stored under aqueous conditions and the solids content of the aqueous suspensions was determined gravimetrically.

TEMPO-mediated oxidation, a widely utilized and studied technique, was performed similar to previous work.[18] Purified biomass (1 g) from soybean hull, wheat straw, wood flour, or as-received Fl-1 Soybean Fiber was added to a solution containing distilled water (100 mL), TEMPO (0.016 g), and sodium bromide (0.1 g). 2.5% NaOCl (14.88 g) solution was then added and the mixture was stirred at room temperature. 0.5 *M* NaOH solution was then added to maintain the solution pH between 10 and 11. Upon pH stabilization, the biomass was collected via filtration (Whatman Qualitative 413) and washed successively with DI water until pH neutral.

Fiber fibrillation was performed using a Microfluidizer High-Shear Processor (Microfluidics Corporation, Newton, MA) type M-110Y equipped with a G10Z Z-type diamond interaction chamber (Genizer, Los Angeles, CA). Inline compressed air, used to feed the intensifier pump, was dried using an SPX Deltech air drier and filter (SPXFLOW, Ocala, FL). A peristaltic pump (Omega Engineering, Stamford, CT) was fitted to

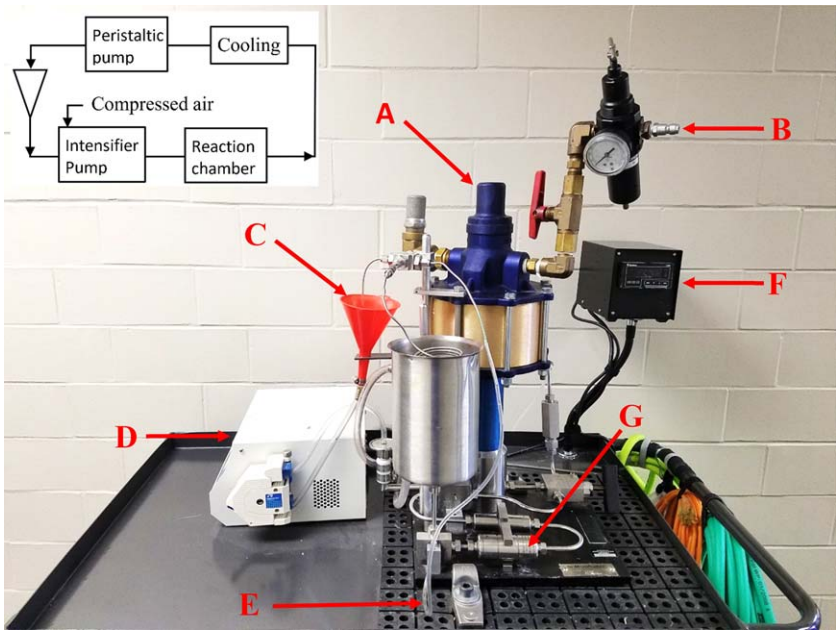

Figure 1. Mechanical fibrillation equipment setup (Microfluidizer High-Shear Processors (Microfluidics Corporation, Westwood, MA). (a) Intensifier pump, (b) inline air supply, (c) processor inlet, (d) peristaltic pump, (e) processor outlet equipped with continuous cooling, (f) interaction chamber pressure monitor, and (g) interaction chamber. The inset shows the flow chart of the nanofibriliation process. [Color figure can be viewed at wileyonlinelibrary.com]

connect the processor inlet (C) and outlet (E) to close the loop. Figure 1 shows a photo of the fibrillation equipment and a flow chart of the nanofibrillation process.

Purified and TEMPO-treated cellulose was prepared in aqueous suspensions (1.5%–2% w/w cellulose content). This suspension was then cycled through the Microfluidizer using the peristaltic pump (D) approximately 5–6 times to undergo fibrillation. Interaction chamber pressure ranged from 8000 to 20,000 Psi during the process and was largely uncontrollable in this range due to inconsistent source flow. Following fibrillation, sodium azide was added to the nanofiber suspension at 0.01% to prevent mold growth and the suspension was stored in a refrigerator for future use.

Preparation of CNF–PEO Nanocomposites

Nanocomposite films containing CNF reinforcement were prepared per the following solvent casting procedure. PEO (3 g) was dissolved in DI water to form a 4% w/w of PEO to DI water solution. The solution was stirred at 60 °C under magnetic stirring for at least 1 hour to ensure full dissolution. CNFs prepared from soybean hull, wheat straw, wood flour, or Fl-1 Soy Fibre were then added at 1%, 3%, 5%, and 7% w/w with respect to dissolved PEO. The mixture was then homogenized using an Ultra Turrax Homogenizer equipped with IKA 25N 25F (IKA, Wilmington, NC) dispersing element at 6000 RPM for 5 min. Air bubbles were removed via centrifugation at 500 RPM for 3 min followed by solution casting on a glass plate. The cast film was then placed in a vacuum oven with a pressure of −80 KPa at 60 °C for 12 h. CNFs from FPL were also used to prepare the nanocomposites in the same manner for comparision.

Atomic Force Microscopy

Atomic force microscopy (AFM) imagining was used to examine the morphology of the CNFs. Silicon wafers were first cleaned by soaking the wafers in a solution of DI water, potassium hydroxide and ammonium hydroxide (5:1:1) at 70 °C for 10 min followed by excessive rinsing by DI water. A drop of diluted CNF suspension was then placed on the cleaned silicon wafers and dried at room temperature. Images of the nanofibers were obtained using atomic force microcopy (AFM, Bruker, D3100, Santa Barbara, CA) tapping mode at 21 °C and 40% relative humidity.

Scanning Electron Microscopy

Scanning electron microscopy (SEM) imaging was also used to examine the morphology of the CNFs. Dilute CNF suspension was dried on glass coverslips, attached to cylindrical aluminum mounts using high-purity silver paint (SPI Products, West Chester, PA) and coated with carbon in a high-vacuum carbon evaporative coater (Cressington 208 C, Ted Pella Inc., Redding, CA). Images were obtained with a JEOL JSM-7600 F SEM (JEOL USA, Inc., Peabody, MA).

Fourier Transform Infrared Spectroscopy

Fourier transform infrared spectroscopy (FTIR) was utilized to study and confirm chemical changes imparted to the cellulose via the TEMPO oxidation technique. A Nicolet 8700 (Thermo Scientific, Waltham, MA) FTIR equipped with a smart iTR attenuated total reflection (ATR) module was used to obtain each spectrum. FTIR spectra were obtained in the range 4000–650 cm^{-1}.

Thermogravimetric Analysis

Thermal degradation characteristics of the chemically modified and fibrillated nanofibers were studied using thermogravimetric analysis (TGA). The thermal degradation characteristics were then compared with commercially obtained CNFs with no surface modification. Thermal stability data for each respective

Table I. Yield Percentages Resulting from Chemical Treatments of Respective Biomass

Chemically treated fibers		
Biomass type	Treatment yield (%)	Mass loss (%)
Pine wood flour	70.8	29.2
Soybean Hull	22.1	77.9
Wheat Straw	41.4	58.6

biomass sample was collected using a TGA Q 500 series Thermo-gravimetric analyzer (TA Instruments, New Castle, DE) using a heating rate of 10 °C/min up to 700 °C under a nitrogen environment.

Mechanical Properties

Tensile properties were examined in accordance with ASTM D882–12. The nanocomposite films were cut into 50 × 5 mm test specimens and each end was taped using Scotch masking tape. The samples were tested using an Instron universal tester (5545, Instron, Norwood, MA) equipped with a 200 N load cell. The samples were held in the grips using custom rubber inserts, which were slightly compressed around the taped ends of the samples after the grips were tightened. The slightly modified gripping method was necessary to avoid the ductile samples from slipping out of the standard grips. All tests were conducted at room temperature with a crosshead speed of 200 mm/min. At least 5 specimens for each nanocomposite film were tested. The average value of each tensile property and its standard deviation were then calculated and reported.

RESULTS AND DISCUSSION

CNF Chemical Composition and Morphology

Hemicellulose and lignin were removed from the biomass during the chemical purification and TEMPO treatment processes. Table I presents the yield percentage (percent of recovered biomass from chemical treatment process) for each biomass after all of the treatment stages for each respective type of biomass. These values are compared to commonly reported biomass chemical compositions for the respective biomass types provided in Table II.

When compared to the original percentage of cellulose in the wood flour (Table II), the yield percentage for the material (Table I) indicates that there is still residual lignin/hemicellulose remaining although the loss of approximatly 29% of the starting mass is likely due to the removal of lignin. A yield percentage of only 22% for soybean hull suggests that the alkali/acid/alkali treatments likely removed both lignin and hemicellulose, and cellulose was also partially degraded and removed. In the case of wheat straw, the yield percentage was greater than the percentage of cellulose present in pristine wheat straw. This is indicative that residual hemicellulose and/or lignin are still present in the final product.

Table II. Lignocellulosic Compositions Reported in Literature for the Three Types of Biomass[8,19]

	Theoretical constituent makeup		
Biomass type	Cellulose (%)	Hemicellulose (%)	Lignin (%)
Pine wood flour	45–50	25–35	25–35
Soybean Hull	56	12.5	10
Wheat Straw	30	50	15

The morpholgy of the nanofibers produced from each respective biomass was studied via AFM and SEM imaging. In Figure 2, AFM images of CNFs prepared from soybean hull, wheat straw, and wood flour revealed fibers with fairly uniform diameters. The depth profiles from the section analysis show that the approximate diameter for soybean hull, wood flour, and wheat straw CNFs are 5, 3, and 6 nm, respectively. The average length of these CNFs are assumed to be in micron scale due to the fact that the fibers span across the entire length of the image. The SEM image [Figure 2(d)] show Fl-1 Soy Fibre CNFs with uniform diameters of approximately 20–30 nm and lengths again assumed to be up to several microns.

The viscosity of nanofiber dispersion increased significantly following mechanical fibrillation. This is due to increased number and surface area of the CNFs in the dispersion, which leads to stronger fiber–fiber and fiber–water interactions and thus a higher dispersion viscosity.[20,21] Figure 3 depicts a representative sample of the CNFs produced in this study.

The resulting CNF dispersion is also much more transparent when compared to the cellulose before fibrillation. Increased transparency has also been widely reported in studies utilizing TEMPO oxidation. This phenomenon is attributed to the significant reduction in CNF diameter made possible by utilizing TEMPO oxidation. Smaller particle size reduces light diffraction thus allowing more light to freely pass through the material, thus increasing transparency.[20]

Modification to the technique previously presented by Alemdar *et al.* was necessary due to the assumed degradation of the biomass fines in the initial alkali soak. The authors utilized a 17.5% w/w alkali soak to purify the wheat straw and soy hull biomass in the study.[12] Biomasses in this study prepared via the method by Alemdar *et al.* displayed no viscosity increase upon microfluidization and nanocomposites which included these materials showed no reinforcing effect. Therefore the initial 17.5% w/w alkali soaked was replaced with a 2% w/w alkali soak.

Spectroscopy

FTIR spectroscopy was used to study and confirm surface modification of purified biomass via TEMPO-mediated oxidation. The selective conversion of the C6 hydroxyl to carboxylate under the TEMPO oxidation conditions was confirmed by FTIR. Figure 4 depicts FTIR spectra taken from samples of respective biomasses before and after TEMPO mediated oxidation. The significant absorbance change in the TEMPO treated samples at approximately 1620 cm^{-1} representing COONa stretching vibration indicates the success of the TEMPO treatment.[22] This peak increases significantly in magnitude for all biomass samples. The presence of the significant IR absorbance at approximately 2050–2100 cm^{-1} contained in the wheat straw,

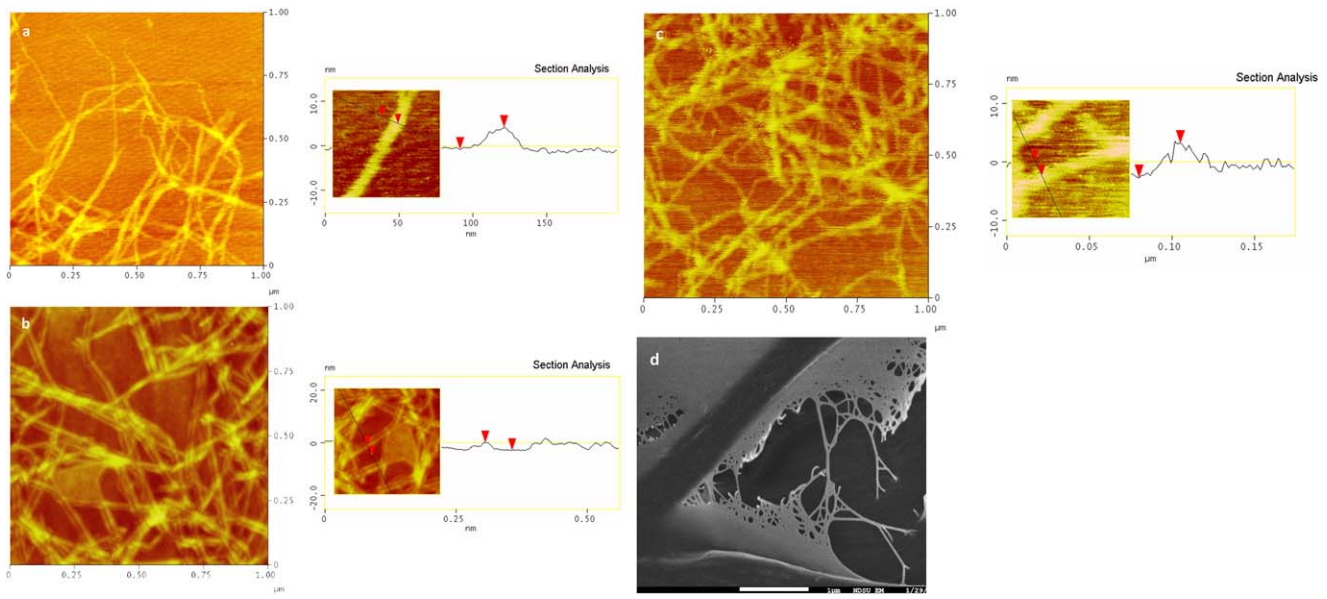

Figure 2. AFM micrographs of (a) soybean hull, (b) wheat straw, (c) wood flour CNFs, and (d) SEM micrograph of Fl-1 Soybean Fibre® CNFs. [Color figure can be viewed at wileyonlinelibrary.com]

wood flour, and Fl-1 Soy Fibre spectrographs is due to the presence of sodium azide in the sample.[23] Sodium azide was added as an antimicrobial agent to prevent mold growth in the samples.

Thermal Stability

Evaluation of thermal characteristics of CNFs is important as they contribute to the reinforcement potential of CNFs for a wide variety of polymeric materials. Many thermoplastic polymers are processed well above 200 °C. Therefore, the effect of chemical, and mechanical treatments on the thermal stability of the fibers was examined via TGA analysis. As shown in Figure 5, unmodified CNFs provided by the FPL display a thermal degradation temperature of approximately 220 °C. TEMPO modified CNFs from the various biomass all behaved similarily and showed the onset of degradation at approximately 205 °C. This change in thermal stability has been attributed to the potential decarboxylation of the surface carboxyl groups at approximately 200 °C, which agrees well with the previouse study by Alemdar *et al.*[12] Such a mild decrease in thermal stability could be potentially undesirable for certain polymers whose processing or service temperatures are close to or above 200 °C.

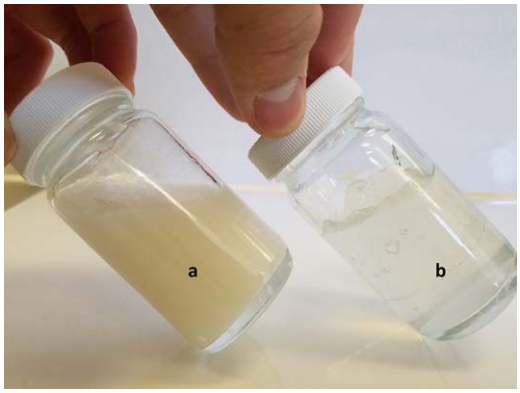

Figure 3. Representative CNF samples (a) before and (b) after nanofibrillation. [Color figure can be viewed at wileyonlinelibrary.com]

Mechanical Properties of CNF–PEO Nanocomposites

Mechanical properties of the PEO–CNF nanocomposites were studied via tensile testing. CNFs should represent significant potential as a reinforcement constituent due to their strong mechanical properties and large aspect ratio. This potential could lead to a new wave of high performance materials which utilize CNFs as reinforcement. Therefore it is important to study the impact that CNFs can have on mechanical properties when used as a reinforcing fiber. Tensile modulus, yield strength, fracture strength, and fracture strain data were collected and tabulated to determine the reinforcement potential of the CNFs in the PEO matrix. These results are graphically shown using the line charts in Figure 6. Table III summarizes these properties including their standard deviations.

Figure 6 shows that CNFs have a profound effect on the mechanical properties of the composites at low nanofiber contents. The yield strength was found to increase with increasing CNF content regardless of the CNF type [Figure 6(a)]. It appears that the strengths of the FI-1 soy and the wood flour CNFs peak at 5 wt % CNF content while the strengths of the soybean hull and the wheat straw CNFs continue to increase at 7 wt % CNF content, although the nanocomposites with higher contents of CNFs should be tested to confirm this trend. The highest strength increases (compared with neat PEO) are 84%, 72%, 103%, and 63% for FI-1 soy, wood flour, soybean hull, and wheat straw CNFs, respectively. It worth noting that all these CNFs lead to higher strength increases of the nanocomposites than the widely used wood pulp-based CNFs (i.e., FPL CNFs), indicating the advantages of the biomass resources and the methods used in this study.

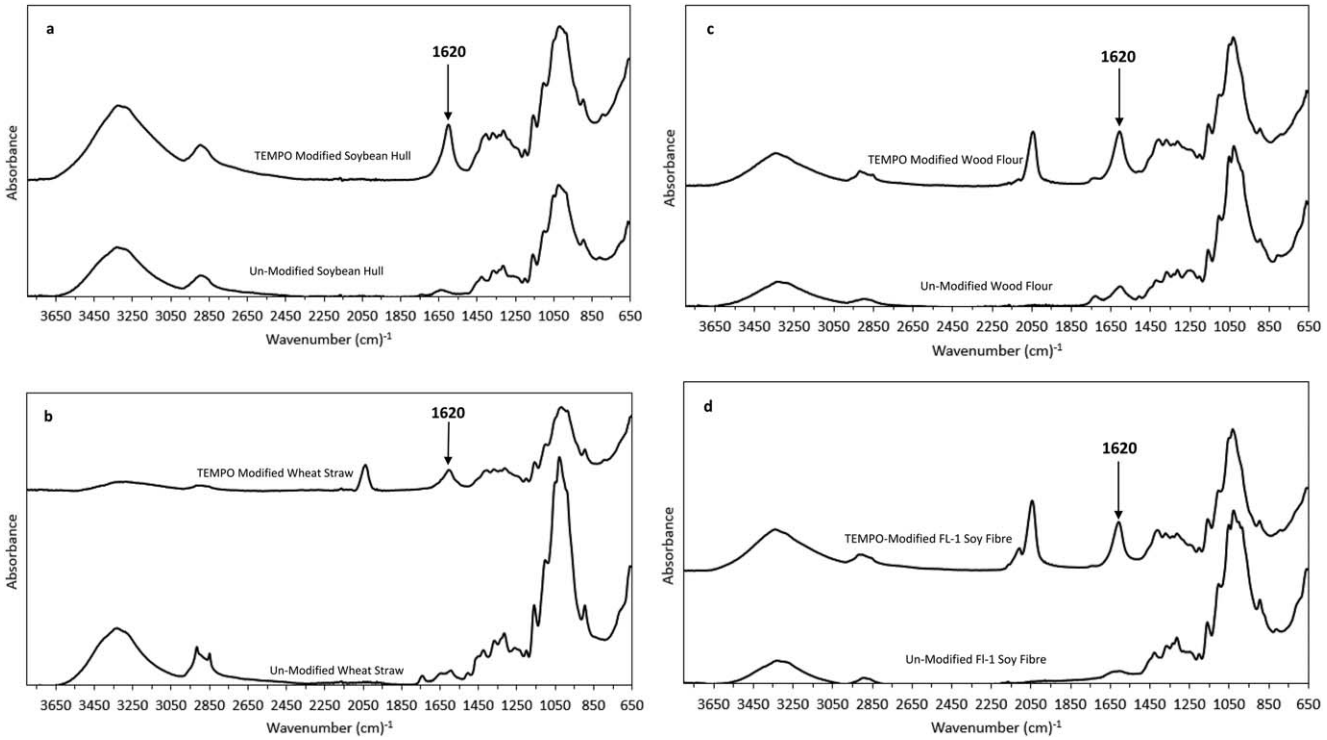

Figure 4. FTIR spectra of un-modified and TEMPO modified (a) soybean hull, (b) wheat straw, (c) wood flour, and (d) Fl-1 Soy Fibre.

A similar increasing trend was observed in the modulus of the nanocomposites reinforced by all types of CNFs [Figure 6(b)]. CNFs produced from soybean hull and wood flour show much higher modulus increases (154% and 147% increase at 7 wt %, respectively) than that of FPL CNFs (85%). The modulus increases caused by Fl-1 soy CNFs is comparable to that of FPL CNFs under most CNF contents (the former is much higher at 7 wt %). The wheat straw CNFs are the only material that imparts smaller modulus increases to the nanocomposites compared to FPL CNFs.

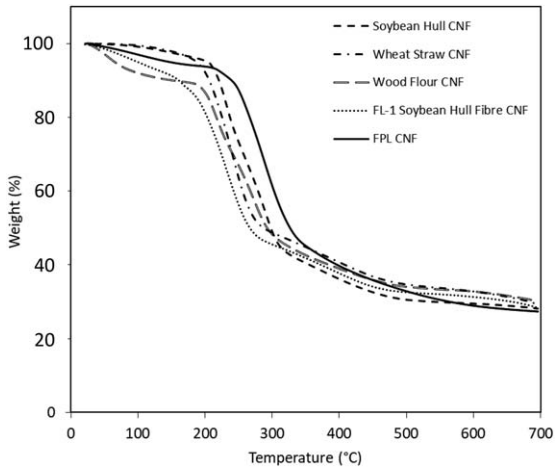

Figure 5. TGA thermograms of CNFs produced from Fl-1 Soy Fibre, soybean hulls, wheat straw, wood flour, and as-received CNFs from the USDA Forest Product Laboratory. The FPL CNFs were not TEMPO treated while all the others were TEMPO treated.

The increases in yield strength and modulus observed are due to the inclusion of CNFs in the PEO matrix. CNFs are much stronger and stiffer than the surrounding PEO matrix and can share a significant percent of load (from the matrix) through interface stress transfer.[21] Additionally, the ability of the CNFs to disperse homogenously to form a network is of significant importance as this network provides efficient stress transfer through the material.[24] The different reinforcement effects demonstrated by the different types of CNFs are hypothesized to be the results of three influencing factors: nanofiber diameter (aspect ratio), purity, and their dispersion in the PEO matrix. Based on the AFM results, the four CNFs produced in this study show a more uniform diameter (i.e., narrower diameter distribution) and a smaller average diameter compared with FPL CNFs, whose morphology and wide distribution of fiber diameter (6–100 nm) are reported in a previous study. Therefore, it is reasonable to expect the four CNFs to outperform FPL CNFs in reinforcing the polymer based on their diameters. In addition, the positive impact of TEMPO treatment on CNF dispersion in water and CNF-PEO interaction can also contribute to the increase in the nanocomposite mechanical properties. It has been shown that the carboxylate surface chemistry introduced via TEMPO oxidation promotes CNF dispersion in water.[25] Therefore, it would be expected that TEMPO oxidized CNFs would be dispersed homogenously in a water-soluble polymer solution such as the PEO solution. Moreover, the addition of surface carboxylate groups increases surface energy and polarity of TEMPO modified CNFs, thus leading to a stronger interaction between TEMPO modified CNFs and PEO.[26]

However, the impurities such as residual lignin in the CNFs produced in this study can complicate the mechanical property

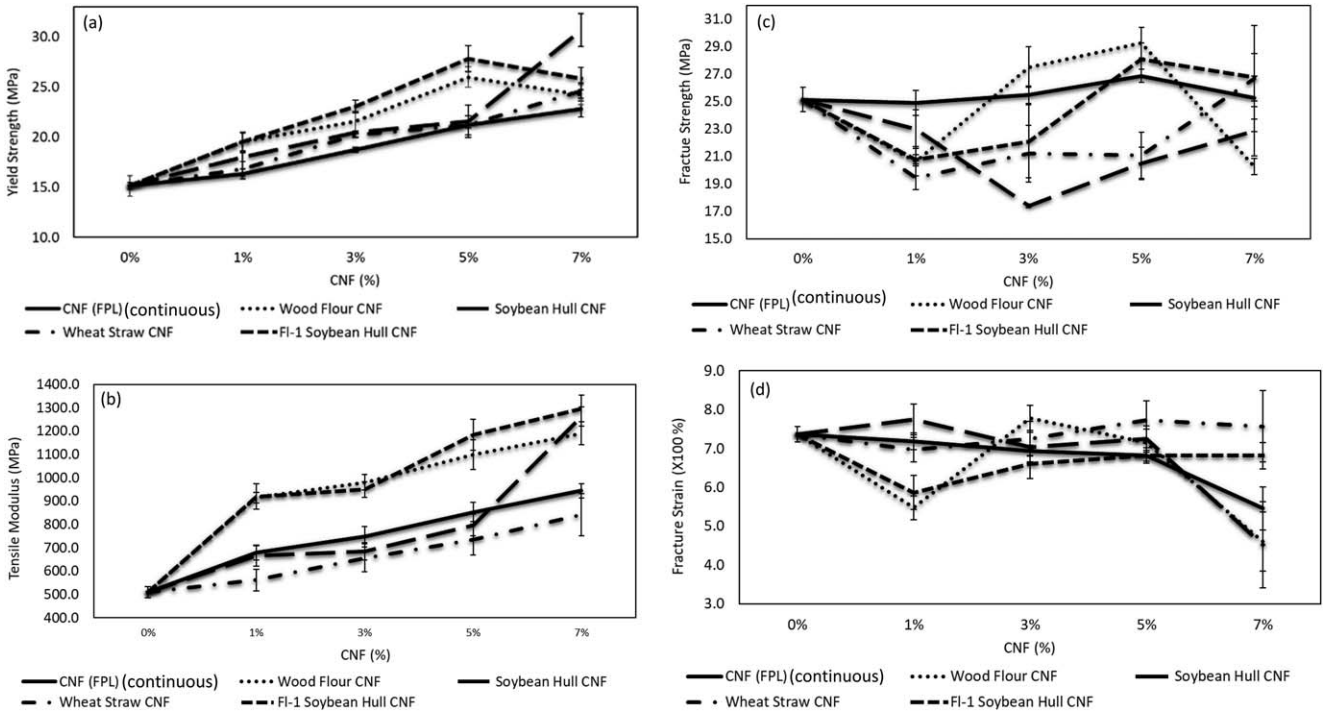

Figure 6. Mechanical properties of PEO nanocomposites reinforced with CNF from various biomass resources. Error bars show standard deviations. (a) yield strength, (b) modulus, (c) fracture strength, (d) fracture strain.

Table III. Mechanical Properties and Their Standard Deviations of PEO/CNF Nanocomposites

		Mechanical properties			
Reinforcement material	% CNF	Tensile modulus (MPa)	Yield strength (MPa)	Fracture strength (MPa)	Fracture strain (X100%)
Neat PEO	0	510.5 ± 23.9	15.1 ± 0.4	25.1 ± 0.9	7.4 ± 0.2
FI-1 Soybean Hull CNFs	1	919.7 ± 53.2	19.5 ± 0.9	20.8 ± 0.3	5.9 ± 0.4
	3	950.1 ± 33.4	23.0 ± 0.6	22.1 ± 2.6	6.6 ± 0.4
	5	1183.4 ± 66.4	27.8 ± 1.3	28.1 ± 1.2	6.8 ± 0.1
	7	1296.6 ± 57.5	25.8 ± 1.1	26.8 ± 1.7	6.8 ± 0.3
Wood flour CNFs	1	915.5 ± 22.7	19.5 ± 0.4	20.6 ± 1.1	5.5 ± 0.3
	3	980.7 ± 32.5	21.6 ± 0.6	27.5 ± 1.5	7.8 ± 0.3
	5	1099.9 ± 63.7	26.0 ± 0.4	29.3 ± 1.1	7.1 ± 0.3
	7	1189.9 ± 49.5	24.2 ± 0.7	20.3 ± 0.6	4.6 ± 0.8
Soybean Hull CNFs	1	666.0 ± 44.0	18.0 ± 0.5	23.0 ± 1.4	7.8 ± 0.4
	3	685.8 ± 37.2	20.4 ± 0.1	17.4 ± 0.1	7.0 ± 0.4
	5	797.3 ± 47.2	21.6 ± 1.6	20.5 ± 1.2	7.2 ± 0.3
	7	1262.1 ± 40.5	30.7 ± 1.7	22.8 ± 1.8	4.5 ± 1.1
Wheat Straw CNFs	1	561.6 ± 46.2	16.8 ± 0.7	19.4 ± 0.9	7.0 ± 0.3
	3	656.2 ± 59.5	20.2 ± 0.2	21.2 ± 2.1	7.3 ± 0.4
	5	735.9 ± 66.5	21.2 ± 1.0	21.1 ± 1.7	7.7 ± 0.5
	7	841.6 ± 91.1	24.6 ± 0.8	26.7 ± 3.9	7.6 ± 0.9
FPL CNFs	1	679.5 ± 32.3	16.3 ± 0.5	24.9 ± 0.9	7.2 ± 0.2
	3	748.4 ± 44.0	18.7 ± 0.2	25.5 ± 0.6	6.9 ± 0.1
	5	852.9 ± 40.4	21.2 ± 0.4	26.9 ± 0.5	6.8 ± 0.2
	7	944.2 ± 31.0	22.8 ± 0.8	25.3 ± 1.6	5.5 ± 0.6

results. As shown by the CNF composition analysis, both wheat straw and wood flour CNFs still contain residual lignin and/or hemicellulose. How exactly these impurities affect the properties of the nanocomposites (and to which degree) in each system is worth further studies; however, they generally result in decreased composite properties due to their low aspect ratios and low mechanical properties. Therefore, it is our conclusion that the impurities are most likely responsible for the differences observed in the mechanical properties, especially the lower modulus of the wheat straw CNF nanocomposite than the FPL CNF nanocomposite.

Large variations in both fracture strain and fracture strength of the nanocomposites are shown in Figure 6(c,d), which is not surprising because the failures occur at very large strains and they are mostly defect initiated and controlled. The nanocomposite samples display fracture strains which vary both above and below the neat polymer and the FPL CNF nanocomposite sample baselines. Typically, fracture strain increases with the addition of CNF at low reinforcement percentages followed by a significant decrease in fracture strain at increasing CNF reinforcement percentages.[15,27] This behavior is attributed to the agglomeration of the CNFs at higher reinforcement percentages, which increases probability of fracture initiation at the agglomeration locations.[21] Although not obvious in the AFM images shown in Figure 2, we believe there could still be big CNF bundles present in the produced CNFs because the CNF samples for AFM imaging were specially diluted to facilitate the study. The impurities and CNF agglomeration/bundles in the matrix can result in different levels and characteristics of defects in the samples, which leads to the large variations in fracture strain/strength. However, the effects of these defects on yield strength and modulus is much less significant compared to on failure strain/strength due to the fact that the first two values are obtained in a very small strain range (i.e., within the elastic region of sample deformation), where the defects have a relatively small role.

CONCLUSIONS

CNFs were produced from three Midwest agricultural residues (i.e., wheat straw, soybean hull, and Fl-1 Soy Fibre) and wood flour using an integrated chemical and mechanical method. Modification to the alkali soak procedure presented in literature was required to minimize degradation to the cellulose present in the particulate biomass used in this study. CNFs produced via this method, regardless of their biomass sources, showed significantly higher or comparable reinforcement effect (except the modulus of the wheat straw CNF nanocomposite) than the widely used wood pulp based CNFs. Among the four types of biomass, FI-1 soy exhibited the best overall reinforcement while wheat straw showed the poorest. Purity of the produced CNFs was found to be an important factor in controlling the reinforcement effect, especially for failure strain/strength due to their defect related nature. These results indicate that the cellulose purification techniques and mechanical treatments utilized herein can be used to produce high quality CNFs from low value agricultural residues. This could lead to new revenue stream for many crops and their residues. Future work will be focused on tailoring the chemical reaction conditions to improve the purity of the produced CNFs.

ACKNOWLEDGMENTS

The authors thank North Dakota Soybean Bean Council for its financial support. We are also grateful for materials testing and imaging assistance, provided by Chunju Gu of the NDSU Department of Coatings and Polymeric Materials, Gregory Strommen of the NDSU Center for Nanoscale Science and Engineering, and Scott Payne of the NDSU Electron Microscopy Center. Gratitude is also expressed for the support of the Department of Mechanical Engineering, NDSU.

REFERENCES

1. Khalil, H. A.; Davoudpour, Y.; Islam, M. N.; Mustapha, A.; Sudesh, K.; Dungani, R.; Jawaid, M. *Carbohydr. Polym.* **2014**, *99*, 649.
2. Lavoine, N.; Desloges, I.; Dufresne, A.; Bras, J. *Carbohydr. Polym.* **2012**, *90*, 735.
3. Bhatnagar, A.; Sain, M. *J. Reinf. Plast. Compos.* **2005**, *24*, 1259.
4. Brinchi, L.; Cotana, F.; Fortunati, E.; Kenny, J. *Carbohydr. Polym.* **2013**, *94*, 154.
5. Lee, H.; Hamid, S.; Zain, S. *Sci. World J.* **2014**, *2014*, 1, DOI: 10.1155/2014/631013.
6. Dufresne, A. Nanocellulose: From Nature to High Performance Tailored Materials; Walter De Gruyter GmbH: Berlin, Germany, **2012**.
7. Moon, R. J.; Martini, A.; Nairn, J.; Simonsen, J.; Youngblood, J. *Chem. Soc. Rev.* **2011**, *40*, 3941.
8. Siró, I.; Plackett, D. *Cellulose* **2010**, *17*, 459.
9. Alemdar, A.; Sain, M. *Bioresour. Technol.* **2008**, *99*, 1664.
10. Kalia, S.; Dufresne, A.; Cherian, B. M.; Kaith, B.; Avérous, L.; Njuguna, J.; Nassiopoulos, E. *Int. J. Polym. Sci.* **2011**, *2011*, 1, DOI: 10.1155/2011/837875.
11. Hubbe, M. A.; Rojas, O. J.; Lucia, L. A.; Sain, M. *Bioresources* **2008**, *3*, 929.
12. Alemdar, A.; Sain, M. *Compos. Sci. Technol.* **2008**, *68*, 557.
13. Ververis, C.; Georghiou, K.; Christodoulakis, N.; Santas, P.; Santas, R. *Ind. Crops Prod.* **2004**, *19*, 245.
14. Liu, Q.; Lu, Y.; Aguedo, M.; Jacquet, N.; Ouyang, C.; He, W.; Yan, C.; Bai, W.; Guo, R.; Goffin, D.; Song, J.; Richel, A. *ACS Sustain. Chem. Eng.* **2017**, *5*, 6183.
15. Safdari, F.; Carreau, P. J.; Heuzey, M. C.; Kamal, M. R.; Sain, M. M. *Cellulose* **2017**, *24*, 755.
16. Oksman, K.; Aitomäki, Y.; Mathew, A. P.; Siqueira, G.; Zhou, Q.; Butylina, S.; Tanpichai, S.; Zhou, X.; Hooshmand, S. *Compos. Part A: Appl. Sci. Manuf.* **2016**, *83*, 2.
17. Saito, T.; Okita, Y.; Nge, T.; Sugiyama, J.; Isogai, A. *Carbohydr. Polym.* **2006**, *65*, 435.
18. Fukuzumi, H.; Saito, T.; Iwata, T.; Kumamoto, Y.; Isogai, A. *Biomacromolecules* **2009**, *10*, 162.
19. Kumar, P.; Barrett, D. M.; Delwiche, M. J.; Stroeve, P. *Ind. Eng. Chem. Res.* **2009**, *48*, 3713.

20. Isogai, A.; Saito, T.; Fukuzumi, H. *Nanoscale* **2011**, *3*, 71.
21. Xu, X.; Wang, H.; Jiang, L.; Wang, X.; Payne, S. A.; Zhu, J.; Li, R. *Macromolecules* **2014**, *47*, 3409.
22. Jiang, F.; Hsieh, Y.-L. *ACS Sustain. Chem. Eng.* **2016**, *4*, 1041.
23. LibreTexts. Infrared Spectroscopy Absorption Table. Available at: https://chem.libretexts.org/Reference/Reference_Tables/Spectroscopic_Parameters/Infrared_Spectroscopy_Absorption_Table
24. Zimmermann, T.; Bordeanu, N.; Strub, E. *Carbohydr. Polym.* **2010**, *79*, 1086.
25. Saito, T.; Nishiyama, Y.; Putaux, J.-L.; Vignon, M.; Isogai, A. *Biomacromolecules* **2006**, *7*, 1687.
26. Lai, C.; Sheng, L.; Liao, S.; Xi, T.; Zhang, Z. *Surf. Interf. Anal.* **2013**, *45*, 1673.
27. Xu, X.; Liu, F.; Jiang, L.; Zhu, J. Y.; Haagenson, D.; Wiesenborn, D. *ACS Appl. Mater. Interfaces* **2013**, *5*, 2999.